Study of Laser-supported Detonation Threshold Using Graphical Analysis

IEPC-2015-174／ISTS-2015-b-174

Presented at Joint Conference of 30th International Symposium on Space Technology and Science 34th International Electric Propulsion Conference and 6th Nano-satellite Symposium, Hyogo-Kobe, Japan July 4 – 10, 2015

Hirotuki Shiraishi[1] and Yuji Matsumoto[2]

[1]Daido University, Nagoya, 457-8530, Japan
[2]Meitec Fielder Co., Ltd., Tokyo, 107-0052, Japan

Abstract: Laser-supported Detonation (LSD), one type of Laser-supported Plasma (LSP) accompanied by a supersonic flow, is considered as one of the most important phenomena because it can generate high pressure and high temperature, which are essential for laser propulsion systems. Though Laser-supported Combustion-wave (LSC) is also categorized as a LSP wave, the propagation is not adequate to propulsion systems. Therefore whether LSD or not is very important for the propagation of LSP. In the previous study, LSP waves were analysed by Computational Fluid Dynamics (CFD) with Multiply-charged ionization model, which describes an accurate ionization process. In this study, LSD-LSC threshold is investigated by both the positional information and the p-v graphs, derived by the CFD results.

Nomenclature

C_p	=	specific heat at constant pressure[J/(kg・K)]
D	=	propagation velocity of detonation wave [m/s]
D_s	=	effective diffusion coefficient for species s [m^2/s]
E	=	total energy (per unit volume) [J/ m^3]
E_e	=	electronic energy (per unit volume) [J/ m^3]
h	=	enthalpy per unit mass [J/kg]
h_e	=	electronic enthalpy per unit mass [J/kg]
I	=	laser intensity [W/ m^3]
I_0	=	incident laser intensity [W/ m^3]
$\hat{I}$	=	first ionization energy [J/particle]
K	=	absorption coefficient [1/m]
M	=	molecular weight [kg/mole]
n	=	number density [1/(m^3)]
$\dot{n}_e$	=	number density rate of production per unit volume by ionization [1/(m^3・s)]
p	=	pressure [Pa]
p_e	=	electron pressure [Pa]
p_0	=	initial pressure of cold gas [Pa]
Q_B	=	radiative energy rate by bremsstrahlung [W/ m^3]
Q_{IB}	=	radiative energy rate by inverse bremsstrahlung [W/ m^3]
Q_T	=	relaxation term between heavy particles and electrons [W/ m^3]
R_0	=	universal gas constant [8.3145 J/(mole ・K)]

[1] Professor, Dept. of Mechanical Engineering, siraisi@daido-it.ac.jp.

t	=	laser irradiation time [s]
T_0	=	initial temperature of cold gas [K]
T_h	=	heavy particle temperature [K]
T_e	=	electron temperature [K]
u	=	velocity in x direction [m/s]
w	=	mass rate of production per unit volume [kg/(m3s)]
x	=	x direction
ν	=	effective collision frequency for electron and species s [1/s]
γ	=	heat capacity ratio
κ_e	=	frozen thermal conductivity for electronic energy [J/particle]
κ_{tr}	=	frozen thermal conductivity for translational energy of heavy particle [J/particle]
λ	=	wavelength of incident laser beam
ρ	=	density [kg/m3]
ρ_0	=	initial density of cold gas [kg/m3]

Subscripts

e	electron
ea	electron-atom collision
ei	electron-ion collision
h.p.	heavy particle
0	initial cold gas

I. Introduction

LASER propulsion is one of the most promising next generation space propulsion systems. Laser-supported plasma (LSP) is essential for this system because the laser energy is mainly absorbed by hot plasma and then converted to the kinetic energy that is necessary for propulsion. In this study, we investigate the use of laser supported detonation (LSD), a type of laser supported plasma (LSP), in a repetitively pulsed (RP) laser propulsion system. LSD is also categorized as a type of hypersonic reacting flow, where exothermicity is supplied by laser absorption than by a chemical reaction.

Raizer [1] examined the energy balance of the LSD and reported that the LSD terminates when the ratio of laser thickness to the diameter of the laser-beam cross section exceeds a certain threshold. With a decrease in the irradiative laser beam intensity by LSD expanding, the detonation can be weaker and transform to laser-supported combustion (LSC) wave, in which the laser absorption zone detaches from the shock front. In an LSC, the shock front propagates almost adiabatically because the heat transfer from the laser absorption zone becomes much weaker. Therefore, the transition from LSD to LSC is a very important topic for laser propulsion systems.

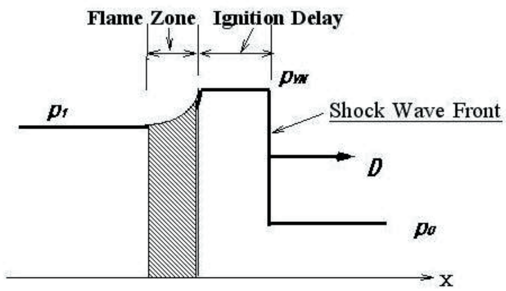

Figure 1. ZND model for chemical detonation.

The most common one-dimensional (1-D) distribution of LSD is the Zel'dovich-von Neumann-Doering (ZND) model. Figures 1 and 2 respectively show a ZND model and p-v diagram of chemical detonation, non-dimensionalized by the initial state. Since both longitudinal axes indicate pressure, direct comparisons can be made.

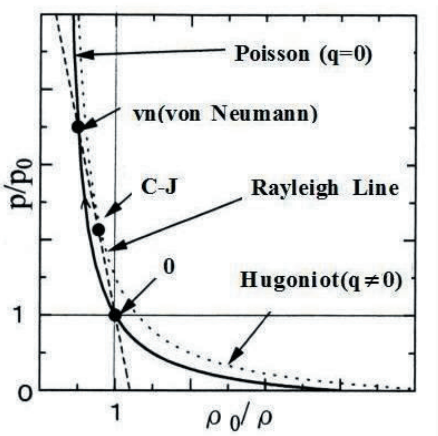

Figure 2. p-v diagram of chemical detonation.

In the diagram, three characteristic lines exist: Rayleigh, Poisson, and Hugoniot curves. These lines derive from the Rankine-Hugoniot relation, which is defined by the conservation laws of mass, kinetic momentum and energy. The coordinate system in the conservation laws is shown in Fig. 3.

The difference between the Poisson and the Hugoniot lines is the heat release value q [J/m3]. The Hugoniot line is calculated as follows:

$$\frac{\gamma}{\gamma-1}\left(\frac{p}{\rho}-\frac{p_0}{\rho_0}\right)-q=\frac{1}{2}(p-p_0)\left(\frac{1}{\rho}+\frac{1}{\rho_0}\right) \tag{1}$$

In the Poisson line, where q is equal to zero, the

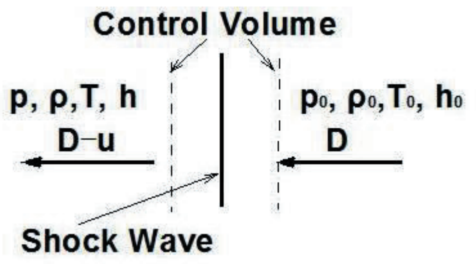

Figure 3. Control volume for conservation laws.

no-heat release case is indicated. The von Nuemann state indicates the ignition delay, where no heat is released by combustion, as shown in Fig. 1.

Figure 4 shows the hypothetical ZND model for LSD. Though the frame zone is displaced by the laser absorption zone, the ionization delay is not clarified because the delay is substantial only near the threshold condition as described in the conclusion of the previous work [2)]. This tendency is exposed only in the multiply-charged model because the ionization delay is exaggerated in the single ionization model [3].

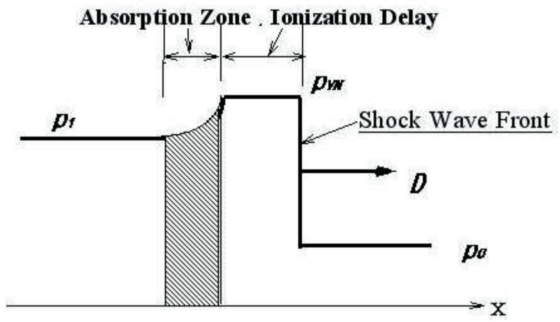

Figure 4. Hypothetical ZND model for LSD.

For simulating LSD propagation, we initially performed 1-D steady and unsteady analyses [4] using a CO_2 gas dynamic laser in argon gas. In this environment, the most important laser absorption mechanism for LSD propagation is the Inverse Bremsstrahlung process: The laser energy is transformed into the kinetic energy of free electrons by photon absorption during collisions of electrons with ions or neutral particles, which is then re-distributed among heavy particles through collisions. As a numerical method, the TVD scheme was applied, which accounts for real gas effects. Though 1-dimensional analyses were performed, the dimension should be extended to the axisymmetric 2-D model [5] for realistic cases.

As a practical case, Wang et al.[6] simulated LSD propagation in the inner geometry of a laser propulsion system. Though some simulations for laser propulsions have been studied, we know of no case that applies a multi-charged model. Therefore, we studied the structure transition near LSC-LSD threshold by applying a multi-charged model to the physical-fluid dynamics scheme that has been constructed for simulating unsteady and non-equilibrium LSD waves propagating through an inert gas, as in the previous work [2]. The lengthened delay of ionization is the most remarkable feature, which indicates the condition of the LSC-LSD threshold.

The objective of this study is to clarify the LSD propagation structure by applying a p-v diagram to the simulation results. This will help us determine whether the difference between the true distribution of LSD and the hypothetical ZND model, as shown in Fig. 4, is important.

II. Numerical Model and Assumptions

A. Analysis model

Figure 5 shows the analysis model for the 1-D study. The CO_2 gas dynamic laser beam (λ = 10.6 μm) passes from the right to the left, and the LSD wave propagates through hydrogen gas at room temperature (T_0 = 300 K). In order to simulate the laser-supported plasma, a hot spot in which hot electrons are seeded, is set up to imitate the initial plasma. This hot spot model imitates the hot electrons, which are generated on a metal target by dielectric breakdown in a previous experiment [7]. In this study, the hot spot is placed at the

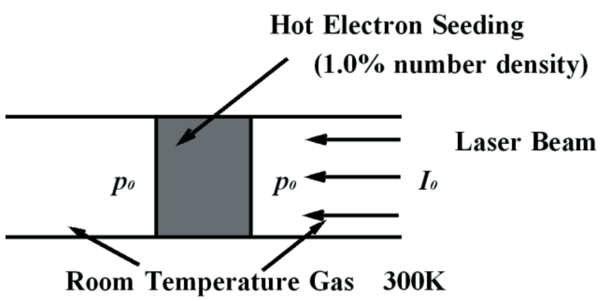

Figure 5. One-dimensional analysis model.

center at x = 2 mm. The hot electron temperature is 15,000 K, and the size of the hot spot is 2 mm (200 points × 0.01 mm). We used a 1% seeding rate because the number of seeded electrons has little effect on the LSD propagation results.

B. Assumptions

The assumptions for this analysis are the same as in the previous work [2]. They are as follows:

(1) The propellant gas is always electrically neutral.

(2) The chemical reactions considered in this model are as follows:

1) $Ar + e^- \leftrightarrow Ar^+ + e^- + e^-$,

2) $Ar^+ + e^- \leftrightarrow Ar^{++} + e^- + e^-$

(3) The thermal non equilibrium model is a two-temperature model, where the electron temperature related to the electron-electronic excitation mode is separated from the heavy particle temperature related to the other modes.

(4) With respect to the effective diffusion coefficient, ambipolar diffusion is also considered.

C. Governing equations

In this study, 1-D Navier-Stokes equations are changed into finite-difference equations, using the TVD scheme, where the radiative energy transfer terms $Q_{\rm IB}$, $Q_{\rm B}$, and $Q_{\rm EE}$ are treated implicitly.

The governing equations are as follows:

$$\frac{\partial \boldsymbol{U}}{\partial t} + \frac{\partial \boldsymbol{F}}{\partial x} = \frac{\partial \mathbf{F}_{\rm v}}{\partial x} + \mathbf{S} \,, \tag{2}$$

where

$$\mathbf{U} = \begin{pmatrix} \rho \\ \rho u \\ E \\ E_{\rm e} \\ \rho_i \end{pmatrix}, \quad \boldsymbol{F} = \begin{pmatrix} \rho u \\ \rho u^2 + p \\ (E+p)u \\ E_{\rm e} u \\ \rho_i u \end{pmatrix},$$

$$\boldsymbol{F}_{\rm v} = \begin{pmatrix} 0 \\ 0 \\ \kappa_{\rm tr}\dfrac{\partial T_{\rm h}}{\partial x} + \kappa_{\rm e}\dfrac{\partial T_{\rm e}}{\partial x} + \sum_j D_j h_j \dfrac{\partial \rho_j}{\partial x} \\ \kappa_{\rm e}\dfrac{\partial T_{\rm e}}{\partial x} + \sum_j D_j h_j \dfrac{\partial \rho_j}{\partial x} \\ D_i \dfrac{\partial \rho_i}{\partial x} \end{pmatrix},$$

and

$$\boldsymbol{S} = \begin{pmatrix} 0 \\ 0 \\ Q_{\rm IB} - Q_{\rm B} \\ Q_{\rm EE} + Q_{\rm IB} - Q_{\rm B} \\ w_i \end{pmatrix}. \tag{3}$$

Here, i indicates Ar, Ar^+, e^-, or Ar^{++} in the case of argon.

Further, in the expression for $\boldsymbol{S}$,

$$Q_{\rm EE} = Q_{\rm T} - p_{\rm e}\frac{\partial u}{\partial x} + \frac{E_{\rm e} + p_{\rm e}}{\rho_{\rm e}} w_{\rm e} \tag{4}$$

In this analysis model, relaxation terms between the heavy particle mode and the electrical modes should be developed in relation to the thermal nonequilibrium model for hypersonic flows [8]. Therefore, Q_T is defined by the following equation:

$$Q_T = 2\rho_e \frac{3}{2} R_0 (T_h - T_e) \sum_{i=h.p.} \frac{\nu_{e,i}}{M_i} - \sum_{i=ion} \dot{n}_{e,i} \hat{I}_i \tag{5}$$

Upon considering real gases, the specific heat C_p and enthalpy h become functions of the temperature, and they can be calculated from the thermodynamic coefficients given by Gnoffo et al. [7] and Matsuzaki [9].

The radiative energy transfer term Q_{IB}, which originates from the Inverse Bremsstrahlung process, is expressed as follows:

$$Q_{IB} = I(x,t) \times (K_{ea} + K_{ei}) \tag{6}$$

where K_{ea} and K_{ei} are given by Kemp et al. [10] and Johnston et al. [11], respectively. Both are functions of the number density, electron temperature, and the wavelength of the laser beam.

The energy loss Q_B is obtained by integrating the expression from zero to infinity with respect to frequency.

$$Q_B = 1.426 \times 10^{-40} n_e n_i T_e^{1/2} \left[\mathrm{W/m^3} \right] \tag{7}$$

These chemically reacting gas dynamic equations with strong source terms are solved using the semi-implicit Harten-Yee nonMUSCL modified flux-type TVD scheme, in which the radiative energy transfer terms Q_{IB} and Q_B and the relaxation term Q_T are treated implicitly.

D. Laser absorption model

In the presence of absorption, the local radiation intensity $I(x, t)$ is governed by the following equation:

$$\frac{dI(x,t)}{dx} = I(x,t) \times (K_{ea} + K_{ei}) \tag{8}$$

III. Results and Discussion

A. Initial conditions

The physical conditions for analyses are given in Table 1.

Table 1. Initial conditions for analyses.

Laser beam intensity	Pressure of cool gas
I_0 = 4.7 – 8.0MW/cm^2	0.25atm

Figure 6 shows the transition of the ionization delay length by the laser intensity after the time of propagative stabilization. The length is defined by the two intersection points of the axis and two tangential lines, which are tangential to the electronic and the atomic number density distributions. In this figure, the delay is substantial only near the threshold condition. Therefore, the lengthened delay of ionization is the most remarkable feature which indicates the condition of the LSC-LSD threshold [2]. In addition, the plot point cannot exists in the case of LSC, because the axial gap has not a steady state.

However, the delay remarkable point is difficult to decide by this graphic. Therefore two cases in the flat region, for example (a) I_0 = 5.6MW/cm^2 and (b) I_0 = 5.45MW/cm^2, should be evaluated more precisely.

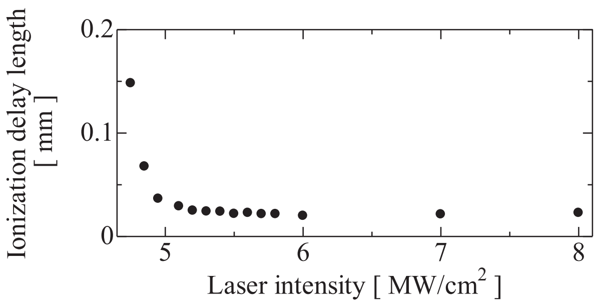

Figure 6. Transition of ionization delay length (p_0 = 0.25atm).

B. Evaluation of LSC-LSD threshold region

Figure 7 shows the p-v diagrams in the case of (a) I_0 = 5.6MW/cm^2, p_0 = 0.25atm and (b) I_0 = 5.45MW/cm^2, p_0 = 0.25atm. Here, we emphasize again that the main object of this study is not the simulation itself, but rather the evaluation of the LSD structure using the simulation results.

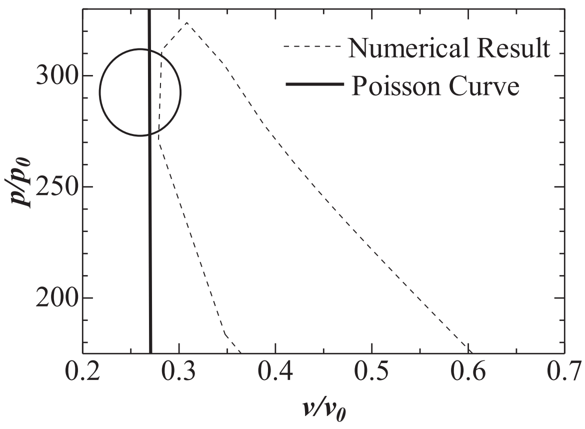

(a) I_0 = 5.6MW/cm^2 (No Touch Case)

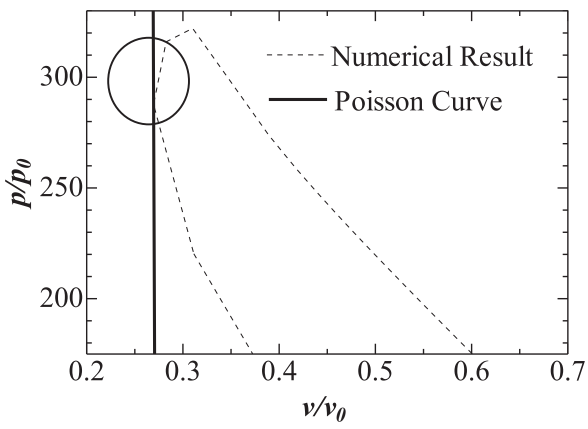

(b) I_0 =5.45 MW/cm^2 (Touch Case)

Figure 7. p-v diagram near LSD-LSC threshold.

In the case of (a), the numerical result does not meet the Poisson curve except at the initial state. According to the p-v diagram in Fig. 2, the laser absorption, which corresponds to the heat release in the chemical detonation, leads to the curve shown in the upper right portion. Therefore, it is clear that laser absorption starts at the previous of the shock front. In contrast, panel (b), the numerical result curve meets the Poisson curve as the same way as in von Neumann condition, which shows a delay in Fig. 2. This indicates that ionization delay exists and that laser absorption does not start at the shock front. The ionization, which produces laser absorption by the inverse-Bremsstrahrung process, delays in the LSC-LSD threshold as well as the hypothetical ZND model for LSD shown in Fig. 4.

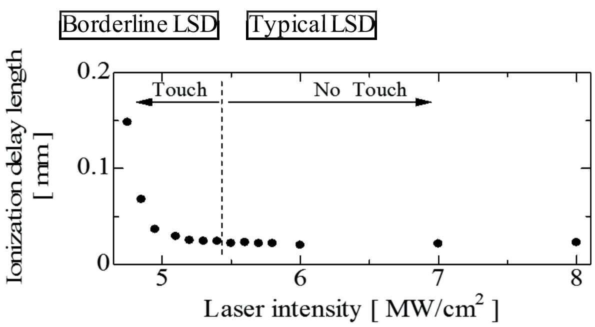

Figure 8. The results of "touch" and "no touch".

Figure 8 shows the transition of the ionization delay length again. The region can be divided into two parts using the p-v diagrams discussed above, which is difficult by the previous procedure [2]. As a result, it is rather rational to rename the "No Touch" and "Touch" to "Typical LSD" and "Borderline LSD", respectively.

IV. Conclusion

In order to study the transition structure from LSD to LSC propagation, a p-v diagram is prepared by l-D simulation by applying the multiply-charged ionization model. The conclusions are as follows:

(i) The p-v diagram clarifies the structure of laser absorption because the same explanation of the heat release as in the case of chemical detonation, which is induced by the Rankine-Hugoniot relation, is applicable.

(ii) Though the ionization delay length appears only in the LSC-LSD threshold as studied in the previous case, it is difficult to decide the precise threshold condition by a simple plotting. Therefore the p-v diagram with Poisson curve are also essential to investigate Borderline LSD region, which exists between the typical LSD and LSC.

References

[1]Raizer, Y. P., "Laser-induced Discharge Phenomena," *Consultants Bureau*, New York, 1977.

[2]Shiraishi, H. and Kumagai, Y., "Numerical Analysis of Threshold between Laser-supported Detonation and Combustion Wave using Thermal Non-Equilibrium and Multi-charged Ionization Model," *Transactions of the Japan Society for Aeronautical and Space Sciences, Aerospace Technology Japan*, 10 (2012), pp.Pb_59-Pb_63.

[3]Shiraishi, H., "Numerical Analysis on Thermal Non-equilibrium and Multidimensional Laser-supported Detonation Wave using Multiply-charged Ionization Model," *Proceedings of 27th Int. Symp. on Space Technology and Science*, 2009, b-34, pp.1-4.

[4]Shiraishi, H., "Fundamental Properties of Non-equilibrium Laser-supported Detonation Wave," *Proceedings of 2nd Int. Symp. on Beamed Energy Propulsion*, 2003, pp.68-79.

[5]Shiraishi, H., "Numerical Analysis on Laser-supported Plasma for Laser Propulsion Systems," *The Journal of Space Technology and Science*, 23 (2007), pp.20-29.

[6]Wang, T.-S., Chen, Y.-S., Liu, J., Myrabo, L. N., and Mead, F. B., Jr., "Advanced Performance Modeling of Experimental Laser Lightcraft," *Journal of Propulsion and Power*, 18 (2002), pp. 1129-1138.

[7]Stuermer, E. and von Allmen, M., "Influence of laser-supported detonation wave on metal drilling with pulsed CO_2 lasers," *Journal of Applied Physics*, 49 (1978), pp.5648-5654.

[8]Gnoffo, P. A., Gupta, R. N., and Shinn, J. L., "Conservation Equations and Physical Models for Hypersonic Air Flows in Thermal and Chemical Nonequilibrium," *NASA Technical Paper*, 2867, 1989, pp.1-57.

[9]Matsuzaki, R., "Specific Heat and Isentropic Exponent of High Temperature Gases Exact Analytical Expressions," *AIAA Paper*, 80-1532, 1980, pp.1-11.

[10]Kemp, N. H. and Lewis, P. F., "Laser-Heated Thruster Interim Report," *NASA Contractor Report*, NASA CR-161665, 1980.

[11]Johnston, T. W. and Dawson, "Correct values for high-frequency power absorption by inverse bremsstrahlung in plasmas," *J. M. Phys. Fluids*, 16 (1973), p.722.